JOURNAL OF GUIDANCE, CONTROL, AND DYNAMICS
Vol. 34, No. 1, January–February 2011

Equitable Aircraft Noise-Abatement Departure Procedures

Xavier Prats,* Vicenç Puig,† and Joseba Quevedo‡
Technical University of Catalonia, 08034 Barcelona, Spain

DOI: 10.2514/1.49530

This paper deals with the optimization of aircraft noise-abatement departure procedures. A multicriteria optimization strategy is presented, where the fairness of the optimal trajectories is assessed vis-à-vis the different noise-sensitive locations around the airport of study. This equitable optimization is formulated as the minimization of the maximum noise-annoyance deviation regarding all considered locations. This strategy is complemented with an iterative lexicographic optimization algorithm which, in turn, guarantees the Pareto efficiency condition of the final solution. Aircraft operating costs are also considered by neglecting the marginal benefits of noise reduction below a certain threshold value. An application example is shown (as an illustrative case) based on a departure of runway 02 at Girona airport in Catalonia, Spain. The results show the feasibility of this technique, which is intended to be used by procedure designers or airport authorities.

I. Introduction

WHEN designing aircraft-terminal area procedures, several factors must be taken into account, such as obstacle clearance or air traffic management constraints. Noise footprints are also becoming an important indicator to be considered in the design of such procedures. In fact, specific noise-abatement procedures are defined in several airports for either the departure or arrival/approach phases. Moreover, the introduction of area navigation (RNAV) and required navigation performance concepts in terminal airspace will improve the design of such procedures by allowing more flexibility in the route design and by reducing the dispersion of the flight tracks. This paper addresses the computation of such noise-optimized flight trajectories aimed at mitigating the noise exposure over the populated areas around the airport. This optimal guidance problem is a nonlinear, continuous, constrained optimal control problem [1,2], and in recent years, several numerical methods aiming at solving it have been widely spread due to the increase in computational performances of common desktop computers. For an interesting and complete survey of these numerical methods, the reader may refer to [3]. In the present paper, the original infinite-dimensional problem is converted into a finite-dimensional optimization problem by transforming the aircraft dynamics system into a problem with a finite set of variables that are solved by using a parameter optimization method, i.e., with nonlinear programming (NLP) [4,5].

In the particular field of aircraft noise-abatement procedures, trajectory optimization techniques are a subject of extensive research and have also been studied by several authors. For instance, in [6], a tool combining a noise-computation model, a geographical information system, and a dynamic trajectory optimization algorithm is presented. With this tool, optimal noise procedures can be computed. A similar methodology is proposed by Clarke and Hansman [7] and an adaptative algorithm for noise abatement is also explained in [8]. On the other hand, Atkins and Xue [9,10] present a dynamic programming technique for minimizing noise in runway independent aircraft operations. More recently, and exploiting the multistage capability of the tool, RNAV procedures are optimized in [11], offering the possibility to calculate routes that can be programmed into current flight management systems (FMS). Finally, in [12,13] another algorithm, based again on direct collocation methods, is defined, and in [14,15], it is shown how this methodology is implemented and tested onboard an aircraft.

The optimization of noise-abatement procedures is also a nonconvex multicriteria minimization problem. In the general case, these kinds of problems are ill defined due to the interrelation among the objective functions. This means that, if we try to minimize one criterion, we may end up maximizing another one; therefore, an appropriate multi-objective decision-making strategy must be used. Common scalarization (or weighting) techniques present some drawbacks, especially with nonconvexities or with the difficulty that arises when different incommensurable criteria (such as noise and fuel) must be considered at the same time [16]. Another potential issue when dealing with the minimization of noise footprints is the computational burden that is required if wide areas of population are to be considered. Some of the previous works consider just a few singular measurement points where noise is supposed to be minimized. Other studies dealing with big areas of population use relatively coarse measurement grids in order to keep the computational burden within acceptable levels.

In this paper, the authors propose an alternative multi-objective optimization methodology based on egalitarian and lexicographic techniques as devised in previous research (see [17,18]). The main goal of this technique is to guarantee a certain degree of fairness among all the noise-sensitive locations. In addition, this methodology allows us to work with a more precise noise-measurement grid, permitting to assess real-world complex scenarios where several noise- sensitive areas are present. Hence, in Sec. II of this paper, this optimization framework is outlined and the different implemented models are described. Then, Sec. III presents the proposed multi-objective optimization strategy and, finally, an illustrative numerical example is given in Sec. IV, where the departure trajectories for two different aircraft are optimized at Girona airport in Catalonia, Spain.

II. Optimization Framework

Figure 1 summarizes the tool that has been developed with the aim of optimizing departure or approach trajectories. The involved airport, with its surrounding cartography, geography, and meteorological data, defines a scenario that is used to compute a given amount of noise annoyance as a function of the emitted aircraft noise along its trajectory. This value, together with some airliner economic considerations, defines one or several optimization criteria. Then, an

Presented as Paper 2009-6939 at the 9th AIAA Aviation Technology, Integration, and Operations ATIO Conference, Hilton Head, SC, 21–23 September 2009; received 23 March 2010; revision received 17 August 2010; accepted for publication 28 August 2010.

*Assistant Professor, Castelldefels School of Technology (EPSC), Office C3-104, Avenida Esteve Terradas, 5, 08860, Castelldefels. Member AIAA.

†Associate Professor, Systems Engineering, Control and Industrial Informatics Department (ESAII), Office 306, Rambla St. Nebridi 10, 08222 Terrassa.

‡Full Professor, Systems Engineering, Control and Industrial Informatics Department (ESAII), Office 306, Rambla St. Nebridi 10, 08222 Terrassa.

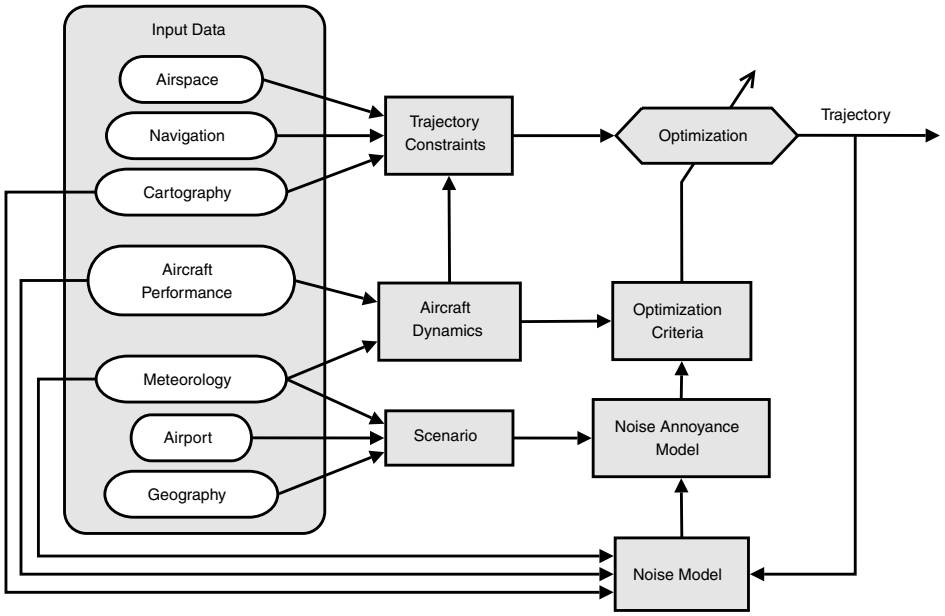

Fig. 1 Optimization framework.

optimization algorithm computes the best departing or approaching trajectory, minimizing these criteria and satisfying a set of trajectory constraints that, in turn, depend on the dynamics of the aircraft, the navigation constraints, and the specific airspace configurations. In this tool, the NLP problem resulting from the discretization of the original optimal control problem is coded by using the general algebraic modeling system (GAMS).[§] Then, the GAMS calls the built-in solver CONOPT[¶] to perform the actual parameter optimization.

This problem can be formally written as a constrained optimal control problem in a given time interval $[t_0, t_f]$. In this case, the value of t_f is left free during the optimization, meaning that it is a decision variable itself that will be fixed by the optimization algorithm. Let $\boldsymbol{x}(t) \in \mathbb{R}^{n_x}$ be the state vector describing the trajectory of the aircraft over the time t, let $\boldsymbol{u}(t) \in \mathbb{R}^{n_u}$ be the control vector that leads to a specific trajectory, and let $\boldsymbol{p} \in \mathbb{R}^{n_p}$ be a set of control parameters not dependent on t. Yet, the time dependency will be dropped from the notation from now on, for the sake of simplicity, in the cases where confusion is not possible. The goal of this problem is to find the best trajectory that minimizes a given set of n_J optimization objectives (or criteria) $\boldsymbol{J} \in \mathbb{R}^{n_J}$, namely,

$$\min_{z \in \mathcal{Z}} \{J_1(z), J_2(z), \ldots, J_{n_J}(z)\} \tag{1}$$

where the admissible set of decision variables $\boldsymbol{z} = [\boldsymbol{x}, \boldsymbol{u}, \boldsymbol{p}, t_f]^T$ is defined as $\mathcal{Z} = L_2(\mathbb{R}, \mathbb{R}^{n_x}) \times L_2(\mathbb{R}, \mathbb{R}^{n_u}) \times \mathbb{R}^p \times \mathbb{R}$, and $J_i(\boldsymbol{z})$ are scalar valued functions representing each individual criterion or objective.

A. Aircraft Dynamics

To derive the equations of motion, the aircraft is treated as a single point of mass. Therefore, only translational motion is considered, neglecting the angular motion of the aircraft [19]. In fact, this assumption means that only the guidance dynamics are considered, since it is assumed that the aircraft would be equipped with autopilots dealing efficiently with the fast rotational dynamics. It is also assumed that turn maneuvers are achieved in a coordinated way (the sideslip angle remaining approximately null), and the aircraft is assumed to fly in a standard atmosphere with calm winds, over a locally flat nonrotating Earth, and with a constant aircraft mass during the departing procedure.

[§]Data available at http://www.gams.com [retrieved October 2010].

[¶]Data available at http://www.aimms.com/aimms/product/solvers/conopt.html [retrieved October 2010].

By using a relative-wind axis formulation, the state vector representing the aircraft trajectory is formed by six components that, for this work, have been chosen as follows:

$$\mathbf{x} = [\, v \quad \chi \quad \gamma \quad N \quad E \quad h \,]^T \tag{2}$$

where v is the true airspeed, χ is the aerodynamic heading yaw angle, and γ is the aerodynamic flight-path angle (FPA). Vector $\mathbf{r} = [\, N \quad E \quad h \,]^T$ represents the aircraft center of mass position, where N and E are the northward and eastward distances, respectively, from a arbitrary chosen origin, and h is the height above this origin (typically the runway threshold). On the other hand, the control vector is chosen as

$$\mathbf{u} = [\, n \quad \mu \,]^T \tag{3}$$

where n is the load factor, and μ is the aerodynamic bank angle. Finally, the control parameters vector is formed by a single component ($\mathbf{p} = [h_c]$), which denotes the height where the thrust cutback is performed. When the aircraft reaches this height, the initial takeoff–go-around thrust configuration is commuted to a climb thrust configuration.

According to the previous considerations, aircraft dynamics are described by the following set of differential equations:

$$\begin{bmatrix} \dot{v} \\ \dot{\chi} \\ \dot{\gamma} \\ \dot{N} \\ \dot{E} \\ \dot{h} \end{bmatrix} = \begin{bmatrix} \frac{1}{m}[T(v,h,h_c) - D(v,n) - mg\sin\gamma] \\ \frac{g}{v}\frac{\sin\mu}{\cos\gamma}n \\ \frac{g}{v}[n\cos\mu - \cos\gamma] \\ v\cos\chi\cos\gamma \\ v\sin\chi\cos\gamma \\ v\sin\gamma \end{bmatrix} \tag{4}$$

where g is the local gravity vector module, m is the mass of the aircraft, and the aerodynamic drag force D is denoted by

$$D(v,n) = \frac{1}{2}\rho S a(v) v^2 + \frac{2mg^2}{\rho S} b(v) \left[\frac{n}{v}\right]^2 \tag{5}$$

where S is the total wing surface, and ρ is the air density that is modeled according to the International Standard Atmosphere (ISA) [20]. The value of aerodynamic coefficients $a(v)$ and $b(v)$ depends on the aircraft flap and slat configuration, where the transition from one configuration to another is usually executed at given operational speeds:

$$a(v) = \begin{cases} a_{\varphi} & \text{if } v \le v_{\varphi\to\varphi-1} \\ a_{\varphi-1} & \text{if } v_{\varphi\to\varphi-1} < v \le v_{\varphi-1\to\varphi-2} \\ \vdots & \\ a_1 & \text{if } v_{2\to1} < v \le v_{1\to0} \\ a_0 & \text{if } v > v_{1\to0} \end{cases} \tag{6}$$

where a_i is the constant aerodynamic coefficient corresponding to the flap/slat configuration i, the operational speed where the transition from configuration i to j is performed is denoted by $v_{i\to j}$, and φ is the total amount of different flap/slat configurations. The aerodynamic coefficient $b(v)$ could be expressed as a function of the same operational speeds in a similar way.

On the other hand, for a takeoff procedure, the total net thrust as a function of time can be expressed by

$$T(v,h,h_c) = \begin{cases} T_{\text{TOGA}}(v,h) & \text{if } h < h_c \\ T_{\text{CL}}(v,h) & \text{if } h \ge h_c \end{cases} \tag{7}$$

where T_{TOGA} is the thrust in takeoff–go-around setting, while T_{CL} corresponds to the climb setting. Since we are dealing with a takeoff, we suppose that, in the whole procedure, the autothrust system is providing the maximum available thrust at a given speed and altitude for each thrust setting. In addition, h_c denotes the height where a thrust cutback is performed. When the aircraft reaches h_c, the initial takeoff–go-around setting is commuted to the climb thrust setting. In this way, we take into account current takeoff operational procedures, where the pilot applies a single cutback at a specified altitude or height.

In a similar way, for an aircraft departure, fuel consumption is modeled as

$$\text{FF}(v,h,h_c) = \begin{cases} \text{FF}_{\text{TOGA}}(v,h) & \text{if } h < h_c \\ \text{FF}_{\text{CL}}(v,h) & \text{if } h \ge h_c \end{cases} \tag{8}$$

where FF_{TOGA} is the fuel flow in the takeoff–go-around configuration, while FF_{CL} corresponds to the fuel consumption in the climb configuration.

Finally, it is worth mentioning that, in order to avoid numerical issues, piecewise Eqs. (6–8) have been approximated with arctangent functions, which are continuous and differentiable and, therefore, more suitable for numerical treatment [18].

B. Noise-Annoyance Model

Here, noise annoyance at different sensitive locations is taken as the principal metric for the noise-impact optimization functions. Noise annoyance mainly depends on the noise level being perceived at a particular location. The same methodology as the integrated noise model (INM) developed by the U.S. Federal Aviation Administration software** is used to compute the noise functions. INM deals with several noise metrics and, in particular, noise levels are computed at a given point by selecting and interpolating appropriate noise values from a noise–thrust–distance table that, in turn, is derived from empirical measurements [21]. INM models provide more accurate contributions to noise propagation, such as weather conditions and cartography, but they are not considered in this paper. However, if implemented, they could be added to the existing framework.

Besides acoustic elements, such as loudness, intensity, spectra distribution, and duration, there are several other elements that need to be taken into account in defining a noise-annoyance figure. Zaheeruddin and Guru [22], Botteldooren et al. [23], and others have shown that noise annoyance can be studied as a qualitative form by using fuzzy logic sets. In previous work, Prats et al. presented how noise annoyance could be modeled by using these techniques in the function of the type of zone being flown over, the maximum noise level, and the hour of the day when then flight is taking place [24]. For this paper, trajectories are supposed to be flown at 10 h, and only residential and industrial zones will be considered. A polynomial function of $L_{\max}$ will define a normalized annoyance index (expressed over the interval [0, 1]), which will be used to build up the optimization functions. Figure 2 graphically shows these functions for the two considered zones.

**Data available at http://www.faa.gov/about/office_org/headquarters_offices/aep/models/inm_model/ [retrieved October 2010].

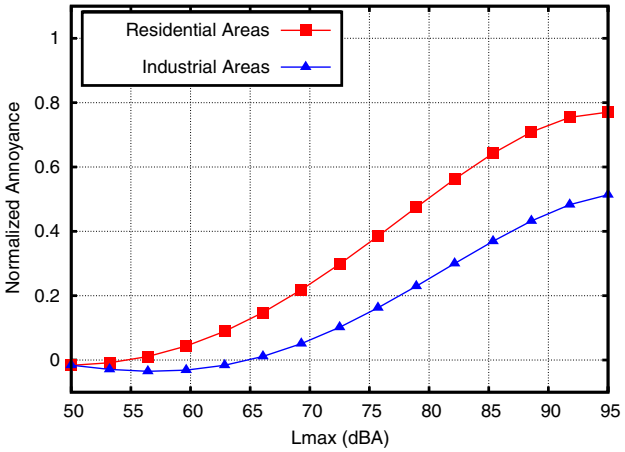

Fig. 2 Representation of the normalized annoyance index in function of $L_{\max}$ at 10 h.

III. Multi-Objective Optimization Strategy

Let $A_i(z)$ be the normalized annoyance index (or just annoyance) at location i for a given trajectory z and at a given hour of the day. Let $A_i^\star$ be the ideal annoyance value at the same location (i.e., as if the minimization of the annoyance at location i was considered as a single objective optimization problem). Then, for the trajectory z, an annoyance deviation at location i is defined as

$$\Delta_i(z) = A_i(z) - A_i^\star \tag{9}$$

These deviations will be used as optimization functions for the problem presented in this paper. Besides noise annoyance, aircraft operating costs will also be taken into account. FMSs, now used on a wide range of aircraft, deal with a compound cost function involving fuel and time consumption during the flight. A cost index parameter (CI) relates the cost of time delay to the price of the fuel and is chosen by an operator before each flight [25]. Thus, this airliner cost function is defined as

$$C_a = \int_{t_0}^{t_f} [\text{FF}(t) + \text{CI}]\,\text{d}t \tag{10}$$

where, by definition, $\text{CI} > 0$ and $\text{FF}(t)$ is the fuel flow in the function of the time.

A. Fairness and Pareto Optimality

When a multi-objective optimization problem is solved, there exists, in general, an infinite set of optimal solutions that are equally acceptable from a mathematical point of view: the Pareto optimal or efficient solutions. A solution z^* of the multi-objective optimization problem, presented in Eq. (1), is said to be Pareto optimal if there does not exist another $z \in \mathcal{Z}$, such that $J_i(z) \le J_i(z^*)$ for all $i = 1, \cdots, n_J$ and $J_j(z) < J_j(z^*)$ for at least one index j. In other words, a solution is Pareto optimal if, and only if, an objective $J_i(z)$ can be reduced only at the expense of increasing at least one of the other objectives. Conversely, a solution z^* is said to be weakly Pareto optimal if there does not exist another $z \in \mathcal{Z}$, such that $J_i(z) < J_i(z^*)$ for all $i \in \{1, \cdots, n_J\}$. Therefore, the Pareto optimal set is a subset of the weakly Pareto-optimal set [16]. Since it is generally desirable to end up with just one final solution, a new element is added in a multi-objective optimization problem, which is a decision-making process. However, this task is not always straightforward, because selecting one solution out of the set of Pareto-optimal ones calls for information that is not contained in the objective functions.

Usually, multicriteria optimization problems are solved by scalarization. Thus, the original problem of Eq. (1) is converted into a single objective optimization problem by forming a linearly weighted sum of the objective functions J_i, namely,

$$\boldsymbol{J}^* = \min_{z\in\mathcal{Z}} \sum_{i=1}^{n_J} w_i J_i(z) \tag{11}$$

The priority of the objectives is reflected by the weights $w_i \geq 0$, which are real numbers and are generally normalized; that is,

$$\sum_{i=1}^{n_J} w_i = 1$$

providing that the different objectives are also normalized. However, choosing the value of the weights is not always a straightforward task. That is why this method is considered in the literature as an a posteriori method, meaning that the decision maker runs several optimizations by changing the values of the different weights, choosing, at the end, the best weight vector that better conforms to what he/she thinks is the best solution. In addition, weighted formulas involve a summation of terms representing different magnitudes, often with very different scales in their units of measurement (such as noise, fuel consumption, or flight time). Prats et al., in [17,26], presented an alternative methodology by using lexicographic optimization, where the different optimization objectives were optimized iteratively according to their relative importance. The most important objective is optimized first, and its optimal value is kept as an additional constraint for the optimization of the second objective, and the algorithm continues iteratively until all the objectives have been minimized.

Yet, when all the criteria share the same priority or importance (such as the noise at different sensitive locations), lexicographic techniques are hard to apply. If scalarization methods are used, it seems obvious to assign the same value to all individual weights ($w_i = 1/n_J \quad \forall\ i \in \{1,\ldots,n_J\}$), minimizing, in this way, the average criterion. Criticisms on this kind of solution were mainly reported by Rawls [27]: despite the fact that the average optimal solution is Pareto efficient, the main concern is that there is no fairness component embedded in this kind of decision-making process. For example, an optimal trajectory where noise annoyance is zero in some locations and extreme in other locations may still be Pareto efficient. Moreover, the average annoyance value may be the minimum one, even if a small minority is actually suffering from extreme annoyance. Summing up, if each location is engaged in minimizing its own annoyance, fairness tends to disappear.

In this context, Rawls [27] formulated an egalitarian principle, stating that a fair system cannot be better off than its worse-off individual. Therefore, if this principle is applied to solve the multiobjective optimization problem of Eq. (1), we have

$$\boldsymbol{J}^* = \min_{z\in\mathcal{Z}}[\max_i J_i(z)], \qquad i = 1,\ldots,n_J \tag{12}$$

Cost functionals of this form have been studied in [28,29] and are already applied to flight optimization in [30] or, more recently, in [5].

B. Multi-Objective Optimization Algorithm

In this work, we propose to give more priority to noise-annoyance minimization than to the minimization of the operational costs. In this way, the trajectory is first optimized regarding only the noise-annoyance impact. Then, the resulting annoyance optimal solution is refined in order to minimize these operational costs by trading off, to some extent, the optimal values of noise annoyance (hierarchical optimization).

1. *Lexicographic-Egalitarian Optimization for Noise Annoyance*

Let us consider now the noise-annoyance minimization problem, where several noise-sensitive locations are taken into account. Let n_L be the total number of these locations (i.e., the total number of points in the measurement grid) and let $\mathcal{L} = \{1,\ldots,n_L\}$ be the set of these locations. As commented on before, the egalitarian technique of Eq. (12) will be used and, for a given hour of the day, this optimization problem is rewritten as

$$\min_{z\in\mathcal{Z}}\{\Delta_1, \Delta_2, \ldots, \Delta_{n_L}\} = \min_{z\in\mathcal{Z}}[\max_{i\in\mathcal{L}}\Delta_i] \tag{13}$$

Note that, for the sake of simplicity, the trajectory dependency z will be dropped from the notation from now on.

The solution of the problem stated in Eq. (13) guarantees fairness, according to Rawls' egalitarian principle, but the obtained solution is weakly Pareto optimal. However, the lexicographic extension of this Rawlsian criterion is indeed Pareto optimal [16,31], and it is adapted in this work. This means that an egalitarian problem, as described in Eq. (13), is solved iteratively, without wasting the solution of the previous iteration step, until a Pareto solution is found. In this way, the solution of this multicriteria optimization technique enjoys both fairness and efficiency properties.

Let $\boldsymbol{\tau}_1$ be the optimal noise-annoyance deviation value obtained from Eq. (13):

$$\boldsymbol{\tau}_1 = \min_{z\in\mathcal{Z}}[\max_{i\in\mathcal{L}}\Delta_i] \tag{14}$$

If, after this optimization, there is no feasible way to decrease the noise annoyance in any location without increasing the $\boldsymbol{\tau}_1$ optimal value, the lexicographic-egalitarian solution is already found, and $\boldsymbol{\tau}_1$ is the Pareto-optimal value of Eq. (13).

On the other hand, in the case that an improvement can still be made in one or more noise-sensitive locations, without increasing the value of $\boldsymbol{\tau}_1$ at some binding locations of the solution of Eq. (14), the problem must continue. Therefore, the next step is to check which noise-sensitive locations can be improved, allowing noise-annoyance deviations below $\boldsymbol{\tau}_1$. Mathematically, location $i \in \mathcal{L}$ is blocked if

$$\min_{z\in\mathcal{Z}}[\Delta_i | \Delta_j \leq \boldsymbol{\tau}_1, \quad \forall\ j \in \mathcal{L}\backslash\{i\}] = \boldsymbol{\tau}_1 \tag{15}$$

Let $\mathcal{B}_1 \subseteq \mathcal{L}$ represent the set of blocked noise-sensitive locations that satisfies Eq. (15), and let $\mathcal{F}_1 = \mathcal{L}\backslash\mathcal{B}_1$ be the set of the remaining nonblocked, or free, locations. As stated previously, if $\mathcal{B}_1 = \mathcal{L}$, the algorithm is stopped due to the fact that all locations are already blocked. Otherwise, the new problem to be solved as a second stage, without wasting the previous solution, is

$$\boldsymbol{\tau}_2 = \min_{z\in\mathcal{Z}}[\max_{i\in\mathcal{F}_1}\Delta_i | \Delta_{j_1} \leq \boldsymbol{\tau}_1, \quad \forall\ j_1 \in \mathcal{B}_1] \tag{16}$$

This procedure is repeated until all noise-sensitive locations become blocked. Then, at the general step $k+1$ of this process, we have

$$\boldsymbol{\tau}_{k+1} = \min_{z\in\mathcal{Z}}[\max_{i\in\mathcal{F}_k}\Delta_i | \Delta_{j_1} \leq \boldsymbol{\tau}_1, \ldots, \Delta_{j_k} \leq \boldsymbol{\tau}_k, \quad \forall\ j_1 \in \mathcal{B}_1, \ldots \quad \forall\ j_k \in \mathcal{B}_k] \tag{17}$$

where

$$\mathcal{F}_k = \mathcal{L}\backslash\left\{\bigcup_{m=1}^{m=k} \mathcal{B}_m\right\}$$

It is worthwhile mentioning that there exists the possibility that, after a given optimization step k, the new set of blocked locations B_k may be empty. This would mean that two or more locations take the optimal value $\boldsymbol{\tau}_k$, but none of them become binding (or blocked). Therefore, the noise annoyance at these locations could be separately reduced while maintaining the remaining objective functions at their optimal value $\boldsymbol{\tau}_k$. In this case, an external decision must be made by artificially blocking at least one location (i.e., by choosing which objective functions can be further improved). This issue, even if mathematically possible, is expected to occur rarely in a real scenario. Should it happen, the decision maker may be aware that he/she is facing two or more equally fair solutions for that problem.

2. Operating Costs Optimization

As mentioned previously, the costs derived from the operation of the aircraft are also considered with the objective function defined in Eq. (10). The iterative process explained previously may end when all optimization criteria become blocked to their best egalitarian value. However, a slight modification is introduced in this loop stopping condition in order to take into account aircraft operating costs. Thus, previous iterations may end as well if the noise annoyances at all the remaining free locations at stage k are below a minimum threshold value of $\bar{A}$. This means that there is no worth in further noise-annoyance reduction below this threshold and some extra freedom is left for the minimization of the airliner cost. Then, as a final optimization step, the airliner cost will be minimized without wasting the optimal noise-annoyance values obtained in the previous solution and will allow them to eventually increase up to this predefined threshold value. At this stage, the user may perform, eventually, some iterations with different values of $\bar{A}$ until an acceptable tradeoff trajectory is found, according to his/her purposes and experience.

Finally, Table 1 summarizes the whole multi-objective optimization strategy that leads to the minimization of the noise-annoyance impact and the flight operational costs.

C. Definition of the Measurement Grid

In real scenarios, areas of population exist instead of a limited set of singular points. A usual way to take populated areas into account is by defining a set of observer locations arranged in the form of a geometric grid of points (see Fig. 3). However, compromises occur between the desired accuracy and the computational burden when solving the optimization problem. Obviously, the larger the size and/or mesh of the grid, the more accurate the solution will be. Yet, it would be more computationally expensive too. A possible solution to improve the computational load would be to manually erase all those points that are not inside a populated area; that is, only consider the circles in Fig. 3. However, with large scenarios, even this approach would be prohibitive if a fine mesh is used. As commented before, a classic approach to solving a multicriteria optimization problem is by using a scalarization function, such as in Eq. (11). If this technique is used, a grid like the one shown in Fig. 3 must be used in order to take into account all observation points to be averaged, and the computational burden becomes an issue.

In this work, a different solution for modeling populated areas is proposed, aiming at considerably simplifying the number of points on the measurement grid. Taking advantage of the lexicographic-egalitarian optimization formulation, we propose considering only those relevant points that produce a significant influence in the optimization process. This task is not straightforward and cannot be formulated objectively. Therefore, we appeal to the common sense or experience of the operator in charge of using the optimization tool. For example, Fig. 4 shows a possible solution for the previous example scenario. If the initial and final points of the trajectory are known beforehand, the operator may guess how the optimal trajectory could be. Depending on the scenario, several equally likely solutions may exist, as is shown in Fig. 4. It is obvious that the optimal trajectory may try to avoid populated areas while respecting the flight dynamics constraints of the aircraft. Then, a distribution of observation points following certain borders of the populated areas closer to the final trajectory would be enough. Since the average noise annoyance is not minimized in this case (as done with classical scalarization techniques), it is not necessary to measure the noise annoyance in the inner parts of the populated areas. There, the acoustical conditions will be better, or at least equal, to those measured in the borders of the area.

Depending on the scenario complexity, this process may not be easy at the beginning, and perhaps some initial trials will be needed in order to adjust the final distribution of measurement points. It is clear that the greater the number of points, the greater the computational burden will be. However, if the distance between two points is too large, the obtained optimal trajectory may fly in between them. This would lead to a virtual optimal solution that would be false, because the noise annoyance in the inner part of the inhabited area has not been considered (see dotted line in Fig. 4). Therefore, the user of this optimization tool should be aware of these possible false solutions, choose (accordingly) the most convenient distribution of measurement points, check the obtained solution, and repeat the optimization if necessary.

Table 1 Lexicographic-egalitarian minimization algorithm for noise annoyance while taking into account operating costs in the last step

1: Initialization:
$k \leftarrow 0$; $\mathcal{F}_0 \leftarrow \mathcal{L}$; $\mathcal{B}_0 \leftarrow \emptyset$
2: **repeat**
3: Perform a constrained egalitarian optimization:
$\mathfrak{T}_{k+1} \leftarrow \min_{z\in\mathcal{Z}}[\max_{i\in\mathcal{F}_k}\Delta_i | \Delta_{j1} \le \mathfrak{T}_1, \ldots, \Delta_{j_k} \le \mathfrak{T}_k, \quad \forall\ j_1 \in \mathcal{B}_1, \ldots, \quad \forall\ j_k \in \mathcal{B}_k]$
4: Determine the set of locations with an optimal value of $\mathfrak{T}_{k+1}$:
$\mathcal{D} \leftarrow \{i | \Delta_i^* = \mathfrak{T}_{k+1}, \quad \forall\ i \in \mathcal{F}_k\}$
5: Determine the new set of blocked locations $\mathcal{B}_{k+1}$:
$\mathcal{B}_{k+1} \leftarrow \{i | \mathfrak{T}_{k+1} = \min_{z\in\mathcal{Z}, i\in\mathcal{D}}[\Delta_i | \Delta_{j1} \le \mathfrak{T}_1, \ldots, \Delta_{jk} \le \mathfrak{T}_k, \Delta_{jk+1} \le \mathfrak{T}_{k+1}, \quad \forall\ j_1 \in \mathcal{B}_1, \ldots, \quad \forall\ j_k \in \mathcal{B}_k, \forall\ j_{k+1} \in \mathcal{F}_k \backslash \{i\}]\}$
6. Update the new set of nonblocked locations:
$\mathcal{F}_{k+1} = \mathcal{L} \backslash \{\bigcup_{m=1}^{m=k+1} \mathcal{B}_m\}$
7: Update step:
$k \leftarrow k + 1$
8: **until** $(\mathcal{B}_k = \mathcal{L})$ **or** $(A_i \le \bar{A}, \forall_i \in \mathcal{F}_k)$
9: **return** Egalitarian solution as $[A_1^*, A_2^*, \ldots, A_{nL}^*]$
10: Minimize the flight operational costs:
$C_a^* \leftarrow \min_{z\in\mathcal{Z}}[C_a | A_i \le \max(\bar{A}, A_i^*) \quad \forall\ i \in \mathcal{L}]$

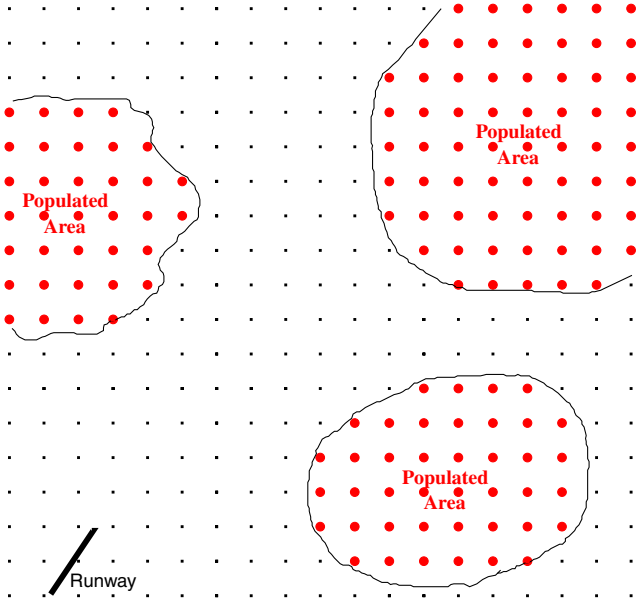

Fig. 3 Example of a regular grid.

IV. Application Example

This section presents some numerical examples based on the east departures from runway 02 at Girona airport in Catalonia, Spain. Two different aircraft are considered for this study, and their relevant data are summarized in Table 2. Moreover, a noise-annoyance threshold of $\bar{A} = 0.25$ has been taken for these examples.

A. Considered Scenario

Nowadays at Girona airport, two standard instrumental departures are published, and both lead to the Begur (BGR) VOR/DME[††]

[††]VOR denotes very high frequency omnidirectional radio range, and DME denotes distance-measuring equipment.

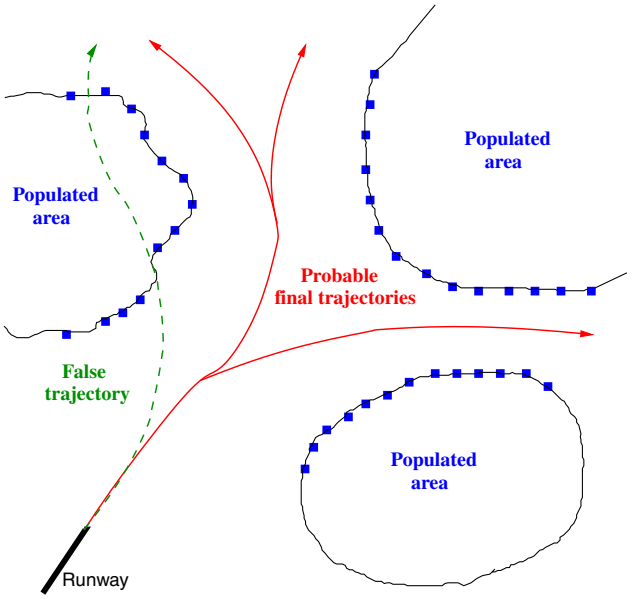

Fig. 4 Example of an ad hoc irregular grid.

facility [32]. These departures overfly the Girona (GIR) VOR/DME facility shortly after takeoff. Then, the aircraft following the departure of BGR2Z perform a right turn to intercept the radial (RDL)-088 of the BGR facility. This departure is used for small- to medium-sized aircraft (such as the Boeing 737 or the Airbus A320), since this turn is limited to a maximum airspeed of 185 kt. Heavier aircraft use the other departure (coded as BGR3G), which continues straight until overflying the Girona NDB[‡‡] (GRN), where the right turn is initiated in order to intercept the RDL-105 of BGR. Both procedures are not noise optimized, and they completely overfly a wide area of population, as seen in Fig. 5. This figure shows the northeast region of the airport where the runway is depicted with a gray strip and is located at the lower left part of the figure. The BGR VOR/DME facility falls well out of the figure, and it is located further east. Moreover, all the residential zones and industrial zones are highlighted.

The populated areas shown in Fig. 5 will be considered in this example. Areas outside of this zone are sparse and, out of this area, the altitude of the aircraft will be high enough that the noise annoyance will be negligible. Therefore, in this scenario, a total number of 119 measurement points are placed irregularly, as explained in Sec. III.C. Among them, 87 points are in residential areas while 32 are in industrial areas. Figure 5 shows the exact location of these measurement points.

B. Trajectory Constraints

In a departure procedure, the initial position of the aircraft is obviously the point where it gets aloft. However, the initial takeoff phase, going from the brake release to the point where the aircraft reaches a height of 122 m (400 ft), is not considered in the optimization process, since the standard operational regulations [33,34] almost restrict all degrees of freedom during this particular phase. In this initial phase, the aircraft follows a straight trajectory, following the departing runway heading at a constant speed (usually the operational V_2 speed), which depends on the aerodynamics and the actual weight of the aircraft. Moreover, during a normal takeoff, the landing gear has been completely retracted when passing 122 m, so it is not taken into account in the dynamical models of both aircraft.

As commented before, the final departure point (BGR VOR/DME) falls well outside of the noise-sensitive area considered for this study. Therefore, with the aim of reducing the computational load of the problem, only the trajectory inside this area will be considered. It is assumed that the remaining segment is flown directly to the VOR/DME facility and, instead of fixing a final point in the trajectory to be optimized, a more general final bound is imposed as follows:

$$E(t_f) \geq 11,000 \text{ m} \tag{18}$$

leaving free the final condition for the north coordinate $N(t_f)$. Then, an additional constraint is added in order to guarantee that the aircraft flies directly from the final point of the optimization to the actual final point of the departure:

$$\chi(t_f) = \begin{cases} \pi - \arctan\left(\frac{E_{\text{VOR}} - E(t_f)}{N(t_f) - N_{\text{VOR}}}\right) & \text{if } N(t_f) > N_{\text{VOR}} \\ \arctan\left(\frac{E_{\text{VOR}} - E(t_f)}{N_{\text{VOR}} - N(t_f)}\right) & \text{if } N(t_f) < N_{\text{VOR}} \\ \frac{\pi}{2} & \text{if } N(t_f) = N_{\text{VOR}} \end{cases} \tag{19}$$

where E_{VOR} and N_{VOR} are, respectively, the east and north coordinates of the BGR VOR/DME.

The remaining bound constraints for the state variables are

$$\begin{aligned} v(t_0) &= V_2, \qquad \chi(t_0) = \chi_{\text{RWY}}, \qquad \gamma(t_0) = \gamma_2 \\ N(t_0) &= N_{400\text{ ft}}, \qquad E(t_0) = E_{400\text{ ft}}, \qquad h(t_0) = 122 \text{ m} \end{aligned} \tag{20}$$

where γ_2 is the FPA that results when the aircraft is flying at V_2 speed while applying takeoff–go-around thrust settings. On the other hand, the origin of coordinates for this problem is placed at the threshold of runway 02. Then, $N_{400\text{ ft}}$ and $E_{400\text{ ft}}$ are, respectively, the north and east coordinates of the point where the aircraft reaches a height of 122 m (400 ft), and χ_{RWY} is the geographic runway heading. All initial/final values of the variables not listed in Eq. (20) are considered free and will be determined by the optimization itself (including the time at the final point t_f).

In addition, and for operational reasons, it is enforced that the speed and altitude of the aircraft should not decrease during the whole departure procedure. Moreover, for the considered scenario, a minimum procedure departure gradient of 5.5% is imposed [32]. Then, these three path constraints are written as

$$\begin{aligned} \dot{\text{EAS}} \geq 0; \qquad \dot{h} \geq 0 \\ h(t) \geq h(t_0) + 5.5/100 \cdot \sqrt{N^2(t) + E^2(t)} \end{aligned} \tag{21}$$

where in first approximation, the equivalent airspeed (EAS) is used as operational velocity (instead of the indicated airspeed). Finally, some variables should be bounded in order to ensure existing operational or safety requirements for a given aircraft. Therefore, the following bounding constraints are also defined for this problem:

$$\begin{aligned} \text{EAS}(t) \leq \text{EAS}_{\max}, \qquad 0.85 \leq n(t) \leq 1.15 \\ -25^\circ \leq \mu(t) \leq 25^\circ, \qquad 244 \text{ m} \leq h_c \leq 915 \text{ m} \end{aligned} \tag{22}$$

where the maximum EAS ($\text{EAS}_{\max}$) may be limited either by an aircraft-related limit (maximum operating airspeed) or eventual airspace constraints (such as the typical restriction of 250 kt below 10,000 ft). On the other hand, in [33] is specified that thrust cutback height should be greater than 244 m (800 ft) for noise-abatement

Table 2 Aircraft data for the application example

	Airbus A340-600	Airbus A321-200
Takeoff mass considered	368,000 kg	77,000 kg
Powerplant	Rolls–Royce Trent 556	IAE V2533-A5
Wing surface	361.0 m^2	122.6 m^2
Initial flap/slat configuration	CONF3	CONF1+F
V_2 speed	94.1 ms^{-1} (183 kt)	78.2 ms^{-1} (152 kt)
Takeoff distance[a]	2440 m	1200 m
CI	70 kg/min	70 kg/min

[a]At ISA conditions.

[‡‡]NDB denotes nondirectional beacon.

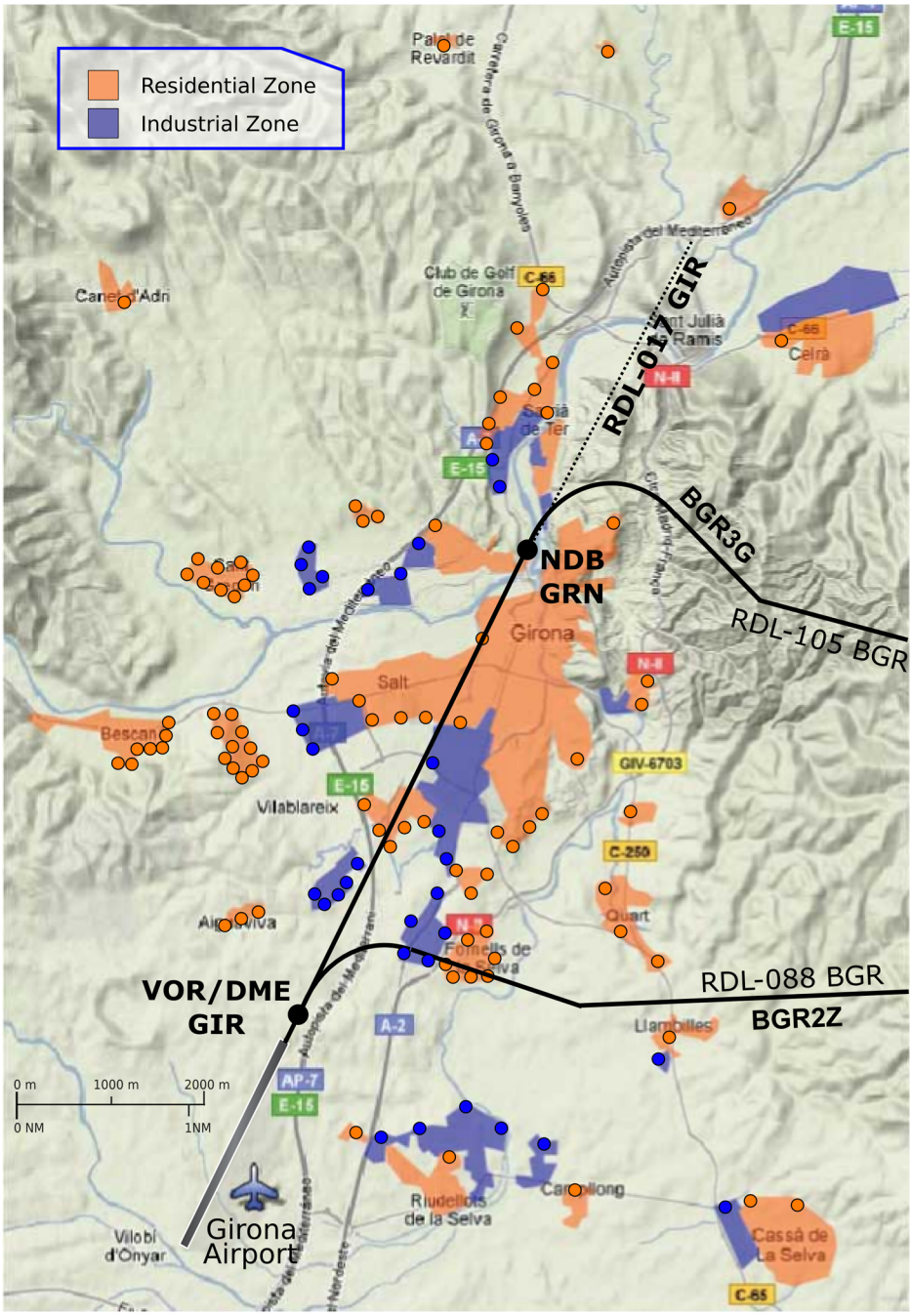

Fig. 5 Considered scenario with the ad hoc measurement grid. (Powered by Google Maps. ©2009 Google. Map data ©2009 Teleatlas.)

purposes. Finally, the load factor n, bank angle μ, and maximum thrust cutback height h_c bounding values correspond to typical values applied by aircraft operators [35].

C. Optimized Trajectories

In this section, the optimal trajectories for both considered aircraft are shown. Being that this problem is nonconvex, we cannot guarantee that a global optimal solution is attained after each optimization step. In fact, the obtained solution may be quite sensitive to the initial variable values (or guesses) that are given at the beginning of the optimization. The NLP solver used in this study allows the user to specify these guess values before running the optimization. To minimize the possibility of being stuck by a local solution, different initial guesses are used before the initial step in the optimization algorithm. The solution that gives the lowest objective value $\mathfrak{J}_1$ is kept. Then, the successive steps in the lexicographic-egalitarian optimization start from the optimal trajectory obtained in the previous step. Yet, after each step, an assessment is done in order to detect possible local optima. This requires, in some cases, the repeat of the optimization at step k with different guesses. Despite being a tedious task, the step-by-step nature of this technique allows the user to check regularly for possible local optima and maximize the probability of ending up with a globally optimal solution in the last step.

1. *Optimal Noise-Annoyance Trajectories: Step-by-Step Example*

To better illustrate how the proposed multi-objective methodology works, the algorithm that derives from Eqs. (13) and (17) is presented step by step in the following example, where the optimization of the Airbus A340 departure is considered. In this first example, the airline operating costs are not considered; therefore, the loop in the algorithm shown in Table 1 will stop once all noise-sensitive locations have been taken into account in the lexicographic-egalitarian process.

As explained in Sec. III.B.1, the first step of the optimization consists of the minimization of the maximum noise-annoyance deviation regarding all locations [see Eq. (13)]. After performing this optimization, an optimal value of $\mathfrak{T}_1 = 0.97$ is obtained, and the resulting trajectory is shown in black (in Fig. 6). After reaching 122 m (400 ft), the aircraft performs an initial left turn in order to avoid the main populated areas and flies in between residential zones A (as marked in the figure). For this example, residential zones A become the binding locations according to the egalitarian principle explained previously [see Eq. (15)]. Then, the trajectory turns right and flies almost directly to the final point.

More precisely, only a few points located at the outer edges of zones A actually bind the restrictions for the next step in the optimization process. Yet, other measurement points located close to these initial binding locations become blocked immediately during the subsequent steps. Therefore, for these successive steps, the obtained trajectory has no appreciable changes if compared with the first step solution, and the successive optimal annoyance deviations take almost the same $\mathfrak{T}_1$ value. However, when all the measurement locations that are located in residential zones A are taken into account as constraints (i.e., all of them become blocked), a significant change is observed in the following step of the algorithm. The trajectory obtained at this second significant step is shown in Fig. 6. Evidently, after overflying locations A, the trajectory continues westward and avoids the residential zone B. The new optimal noise-annoyance deviation becomes $\mathfrak{T}_2 = 0.81$. Then, the third significant step produces a trajectory with an optimal annoyance deviation of $\mathfrak{T}_3 = 0.62$, corresponding to binding locations at zones C, as seen in Fig. 6. The next significant step binds locations D with $\mathfrak{T}_4 = 0.34$ and, finally, the last significant step achieves $\mathfrak{T}_5 = 0.30$, binding locations E. At this stage, all the noise-sensitive locations become blocked; therefore, the obtained solution is Pareto efficient.

Figure 7 shows the time histories of the control variables and the rest of the state variables for this final trajectory, and Fig. 8 shows this trajectory along with the optimal points where the thrust cutback and the flap/slat retraction actions are performed. As seen from these figures, an initial climb is performed at the initial V_2 speed. Then, the thrust cutback is performed, passing from the takeoff–go-around configuration to the climb configuration at 543 m (1780 ft). This reduction is done just before overflying in between locations A, as depicted in Fig. 6. In this initial phase, the high-thrust setting, in combination with the low speed of the aircraft, allows the best climb

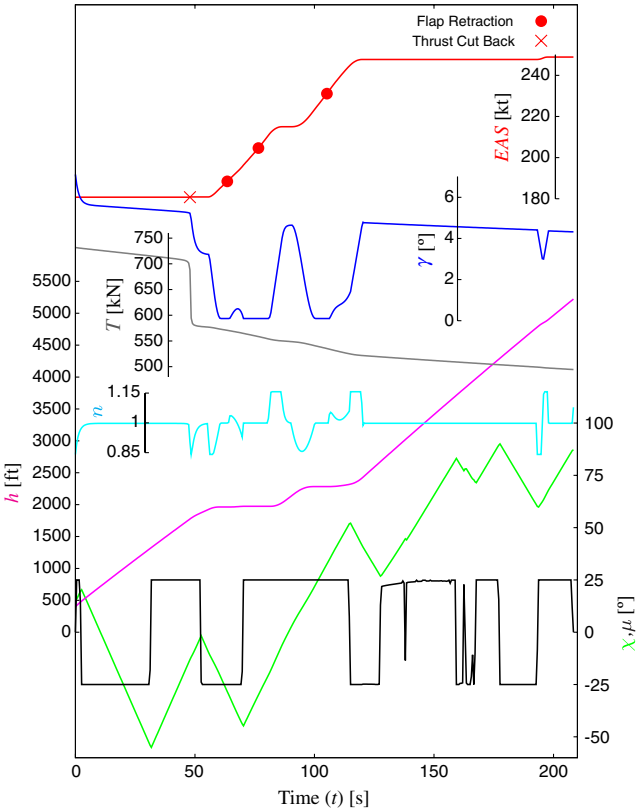

Fig. 7 State and control variables for the optimal trajectory without considering operating costs for the Airbus A340.

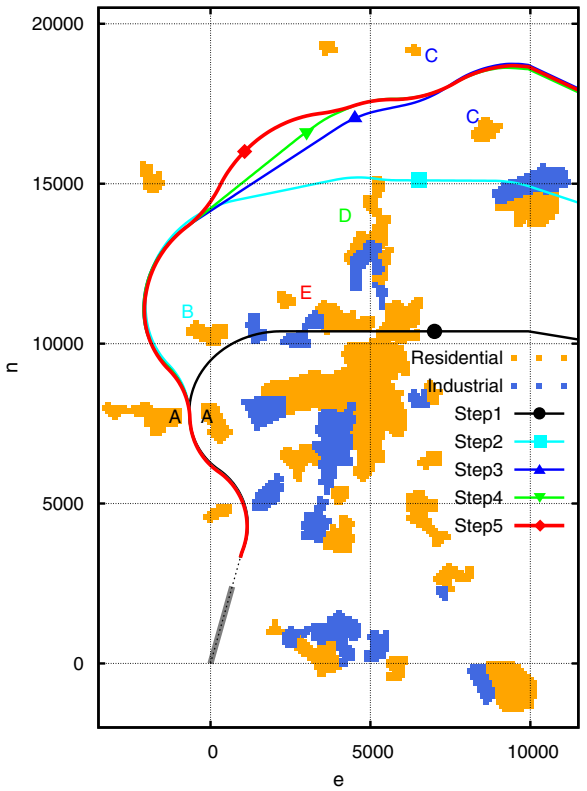

Fig. 6 Significant intermediate steps in the lexicographic-egalitarian optimization algorithm for the Airbus A340 departure.

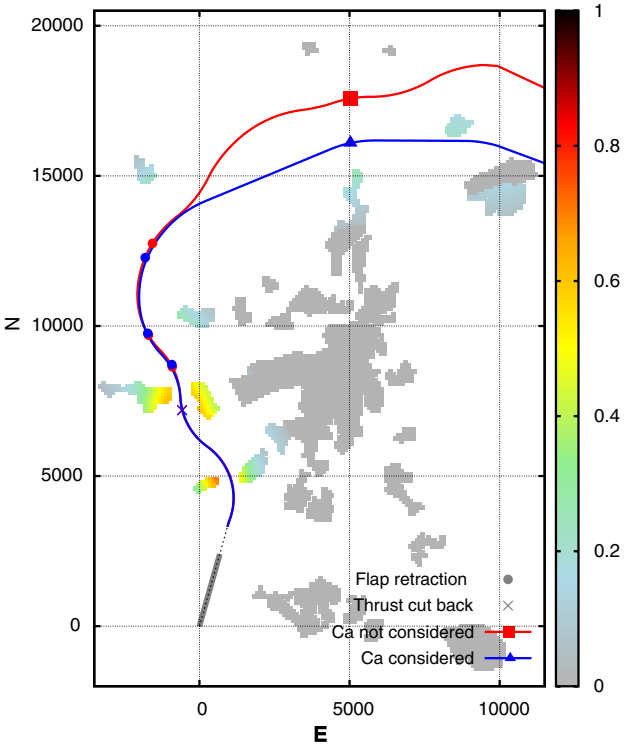

Fig. 8 Optimal trajectories for the Airbus A340. Annoyance map corresponding to the noise annoyance and operating costs optimized trajectory.

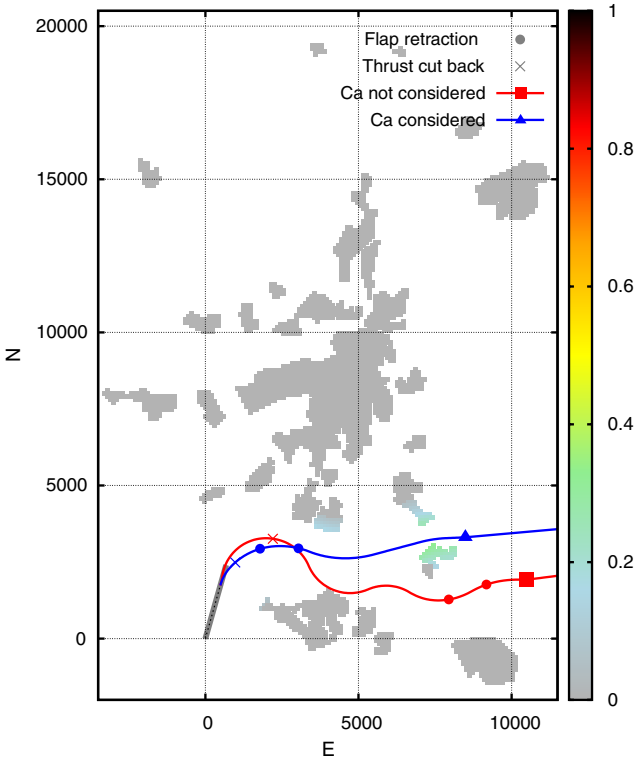

Fig. 9 Optimal trajectories for the Airbus A321. Annoyance map corresponding to the noise annoyance and operating costs optimized trajectory.

performance. In this way, the altitude is maximized when approaching locations A and, in turn, the annoyance is reduced. Besides the altitude, the reduction in thrust just before overflying the inhabited areas decreases the perceived noise at these locations as well. A few seconds after this thrust cutback, the aircraft is leveled off at almost 610 m (2000 ft). This flat segment is used to accelerate the aircraft and to transition successively from the CONF3 to the CONF1 flap/slat configuration. Another short climb follows, improving the annoyance at locations B. When these locations are far enough, a second flat segment at about 700 m (2300 ft) is used again to accelerate to the final climbing speed and adopt the CONF1 flap/slat configuration.

On the other hand, when the same optimization process, as detailed previously, is applied to the Airbus A321 departures, a completely different final trajectory is obtained. Figure 9 shows the

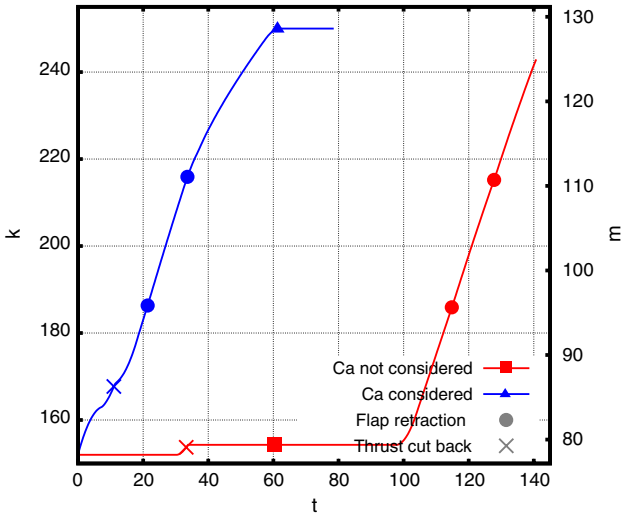

Fig. 11 Optimal speed profiles for the Airbus A321.

optimal trajectory for this aircraft when the operating costs are not considered. Moreover, Figs. 10 and 11 show the vertical and speed profiles for this optimized trajectory. If compared with the A340, the flight performances of the A321 allow an initial tight right turn that permits flying south from the major populated areas. Thrust cutback is performed at about 655 m (2150 ft), just before flying to the next closest residential area. Like in the A340 case, this trajectory also maximizes the initial climb; therefore, a relative low airspeed is scheduled. The acceleration segment (and consequently the retraction of flaps/slats) does not come until all significant populated areas are overflown. Then, a flat segment is used to accelerate and clean the aircraft configuration.

2. *Considering Operating Costs*

Let us now consider the aircraft operating costs, as stated in the original algorithm, shown in Table 1. In this case, the lexicographic-egalitarian process explained previously stops when the noise-annoyance deviations in all nonblocked locations are under the specified threshold level $\bar{A} = 0.25$. Then, the operating costs are minimized while respecting the noise-optimal values at blocked locations and this noise threshold at the remaining locations.

Figure 8 shows the horizontal track for the new optimized trajectory corresponding to the Airbus A340 departure. As seen in the figure, the first portion of this horizontal track overlaps with the previous noise-annoyance optimal trajectory. Shortly after the last

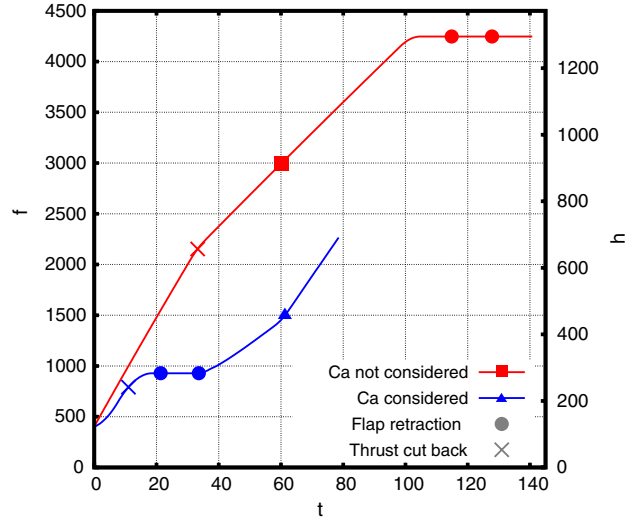

Fig. 10 Optimal vertical profiles for the Airbus A321.

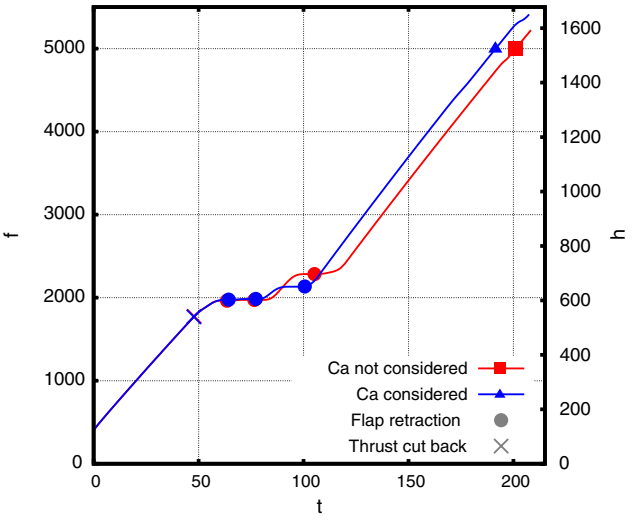

Fig. 12 Optimal vertical profiles for the Airbus A340.

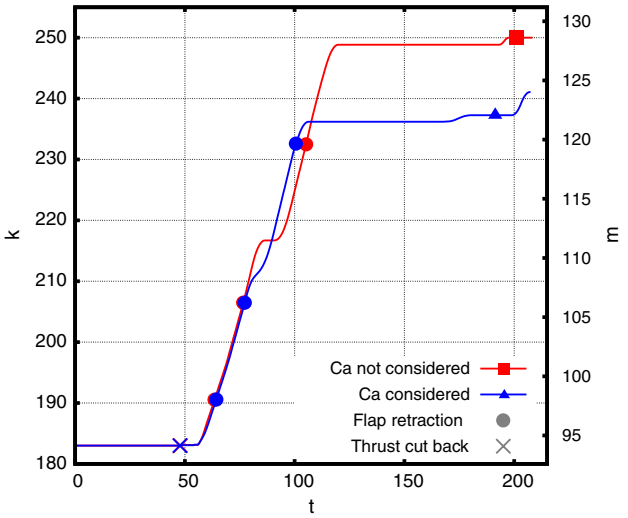

Fig. 13 Optimal speed profiles for the Airbus A340.

Table 3 Operating cost values for the different optimal trajectories (CI = 70 kg/min)

Aircraft	Optimization type	Time	Fuel	C_a
A340	C_a not considered	211 s	1492 kg	1738 kg
	C_a considered	205 s	1450 kg	1689 kg
A321	C_a not considered	141 s	317 kg	481 kg
	C_a considered	79 s	175 kg	267 kg

flap/slat retraction, the new trajectory starts to differ, flying more directly to the final departure fix. The reason for this difference is obviously the consideration of the operating costs in the minimization. This new trajectory improves fuel and time efficiency while not exceeding the maximum annoyance threshold value of 0.25 at the remaining nonblocked locations. Besides the horizontal tracks, Fig. 8 also shows the annoyance values at the different populated areas corresponding to this final trajectory. Once a trajectory is known, the computation of these maps is not a problem from a computational point of view. A regular (equally spaced, rectangular) and more accurate grid is used with a mesh of 100 × 100 m of cell dimension. In addition, when drawing these maps, the size of the pixels has been chosen in order to correctly tessellate the different areas.

When looking at the vertical and speed time histories for this new trajectory, almost no differences are found if compared with those obtained when minimizing noise annoyance. This is due to the fact that the initial part of the trajectory almost restricts all degrees of freedom in how the potential and kinetic energy may be used. As seen in Figs. 12 and 13, a small anticipation of the CONF1+F to CONF1 slats/flaps transition is observed in this new trajectory, because the second flat acceleration segment is almost suppressed and the aircraft has a higher acceleration. However, the final climb airspeed is lower if compared with the noise-annoyance optimized trajectory, leading to a steeper climb profile and allowing, in this way, an improvement in fuel consumption. Table 3 contains the operating costs for this new trajectory along with the original operating costs of the trajectories where only annoyance was minimized.

On the other hand, for the Airbus A321, Figs. 9–11 show the optimal horizontal track and the vertical and speed profiles, respectively. In this case, it is found that the operating-cost minimization notably changes the final trajectory. The horizontal flight path is indeed smoother than in the case where only noise annoyance is minimized. In addition, as seen in all three pictures, the thrust reduction is performed at 244 m (800 ft), which is the lowest possible altitude, reducing (in this way) the fuel consumption. The speed and vertical profiles also change completely if compared with the noise-annoyance optimal profiles. Shortly after the thrust cutback, a short level flight is performed, and the aircraft transitions to clean configuration. This improves climb performance but also minimizes fuel and time consumption. See Table 3 for these numerical values and a comparison with the only annoyance optimized trajectory for this aircraft.

Finally, Fig. 14 shows a three-dimensional view of the these final optimal trajectories for both of the aircraft.

D. Computational Cost

The previous scenario was solved using a common desktop PC, based on an Intel E6600 2.3 GHz processor. According to the output log file of the CONOPT solver, the problem had 179,752 variables and 271,279 constraints. The first step in the lexicographic algorithm required more time to converge than the ones following. In this case, the first optimization steps took an average of 2 h of CPU to converge. Further egalitarian steps required from a few seconds to 30 min., depending on the flexibility left in the optimization. Finally, the airliner cost optimization took an average of 1 h of CPU.

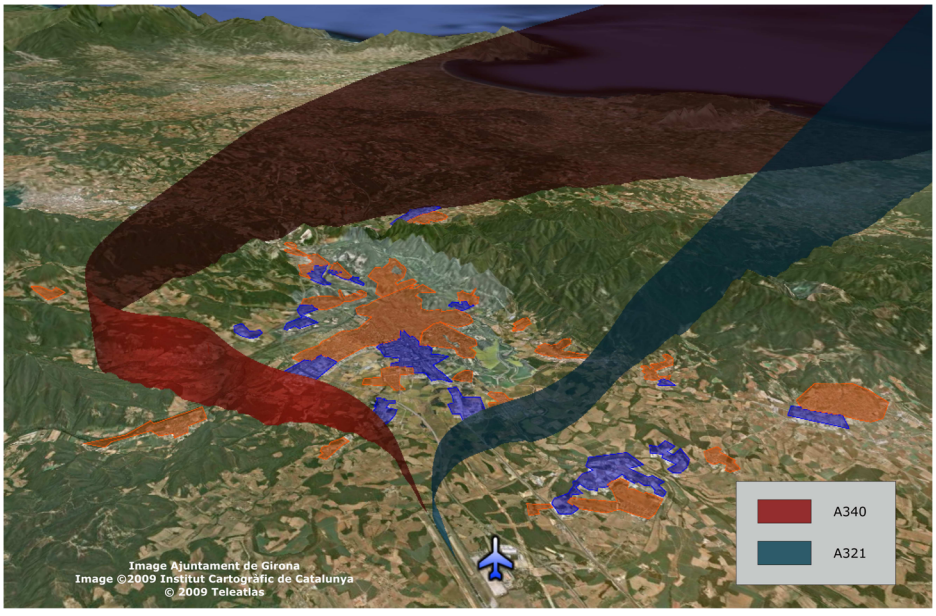

Fig. 14 Three-dimensional view of the final optimal trajectories for both aircraft.

V. Conclusions

In this paper, the authors propose an alternative multi-objective optimization technique that minimizes the noise-annoyance deviation in the worst noise-sensitive location. In this way, the fairness of the final solution is taken into account according to the Rawlsian or egalitarian principles. Moreover, the method is enhanced with an iterative lexicographic algorithm that guarantees that the final solution enjoys both fairness and Pareto efficiency. Aircraft operating costs are also considered as a last step in this optimization process. In particular, noise annoyance is considered infinitely more important than the operational costs, except in those places where annoyance values can be below a given threshold, and some tradeoff between noise-annoyance and these costs is allowed. This methodology permits us to define an irregular and ad hoc grid for the noise-measurement points, which enables us to take into account more accurately the actual population distribution without seriously penalizing the computational load. The feasibility of this technique is shown with some practical examples in a real scenario, where the annoyance of residential and industrial zones is considered. The computational burden required for solving the problem remains at acceptable levels if considering that these kinds of studies would be carried out by airport authorities and/or procedure designers when assessing the operations of a particular airport. The authors believe that the lexicographic-egalitarian technique is a good approach to deal with the multiple noise-sensitive locations, which represent conflicting objectives. Moreover, the consideration of aircraft operating costs is also an important tradeoff that has to be assessed in more detail. In this work, a simple strategy is used in order to decrease these costs at the expense of a slight increase to the overall noise annoyance. Work is underway studying the sensitivity of this tradeoff in order to better assess, for example, the most convenient value of the noise threshold $\bar{A}$. In addition, a deep comparison of this technique with respect to other multicriteria optimization approaches is also foreseen. The presented results can be seen as optimal noise trajectories from a theoretical point of view. Future work will deal with the operational assessment of these trajectories, considering their flyability, safety, and their integration with other procedures already existing in the terminal maneuvering area.

Acknowledgment

The authors wish to acknowledge the support received by the Research Commission of the Generalitat of Catalunya (group SAC, 2009SGR1491).

References

[1] Bryson, A. E., and Ho, Y.-C., *Applied Optimal Control*, Hemisphere, New York, 1975.

[2] Schultz, R. L., "Aircraft Three-Dimensional Trajectory Optimization," *Journal of Guidance, Control, and Dynamics*, Vol. 13, No. 6, Nov.–Dec. 1990, pp. 936–943. doi:10.2514/3.20564

[3] Betts, J. T., "Survey Of Numerical Methods For Trajectory Optimization," *Journal of Guidance, Control, and Dynamics*, Vol. 21, No. 2, 1998, pp. 193–207. doi:10.2514/2.4231

[4] Betts, J. T., and Cramer, E. J., "Application of Direct Transcription to Commercial Aircraft Trajectory Optimization," *Journal of Guidance, Control, and Dynamics*, Vol. 18, No. 1, Jan.–Feb. 1995, pp. 151–159. doi:10.2514/3.56670

[5] Betts, J. T., *Practical Methods For Optimal Control And Estimation Using Nonlinear Programming*, 2nd ed., Advances in Design and Control, Soc. for Industrial and Applied Mathematics, Philadelphia, May 2010.

[6] Visser, H. G., and Wijnen, R. A., "Optimization of Noise Abatement Departure Trajectories," *Journal of Aircraft*, Vol. 38, No. 4, July 2001, pp. 620–627. doi:10.2514/2.2838

[7] Clarke, J.-P., and Hansman, R. J., "A System Analysis Methodology for Developing Single Event Noise Abatement Procedures," Massachusetts Inst. of Technology, Aeronautical Systems Lab., TR ASL-97-1, Cambridge, MA, 1997.

[8] Zou, K. F., and Clarke, J.-P., "Adaptative Real-Time Optimization Algorithm for Noise Abatement Approach Procedures," Proceedings of the 3rd AIAA Aviation Technology, Integration, and Operations (ATIO) Conference, AIAA Paper 2003-6771, Nov. 2003.

[9] Atkins, E. M., and Xue, M., "Noise-Sensitive Final Approach Trajectory Optimization for Runway- Independent Aircraft," *Journal of Aerospace Computing, Information, and Communication*, Vol. 1, No. 7, July 2004, pp. 269–287. doi:10.2514/1.3924

[10] Xue, M., and Atkins, E. M., "Noise-Minimum Runway-Independent Aircraft Approach Design for Baltimore-Washington International Airport," *Journal of Aircraft*, Vol. 43, No. 1, Feb. 2006, pp. 39–51. doi:10.2514/1.15692

[11] Hogenhuis, R. H., Heblij, S. J., and Visser, H. G., "Optimization of RNAV Noise Abatement Arrival Trajectories," *Proceedings of the 26th International Congress of the Aeronautical Sciences (ICAS)*, International Congress of the Aeronautical Sciences Paper 2008-4.11.1, Stockholm, Sept. 2008.

[12] Suzuki, S., Tsuchiya, T., and Andreeva, A., "Trajectory Optimization for Safe, Clean and Quiet Flight," *Proceedings of the 1st ENRI International Workshop on ATM/CNS (EIWAC)*, Electronic Navigation Research Inst., Tokyo, March 2009, pp. 31–35.

[13] Tsuchiya, T., Ishii, H., Uchida, J., Ikaida, H., Gomi, H., Matayoshi, N., and Okuno, Y., "Flight Trajectory Optimization to Minimize Ground Noise in Helicopter Landing Approach," *Journal of Guidance, Control, and Dynamics*, Vol. 32, No. 2, March 2009, pp. 605–615. doi:10.2514/1.34458

[14] Suzuki, S., and Yanagida, A., "Research and Development for Fault Tolerant Flight Control System, Part 1: Intelligent Flight Control System," *Proceedings of the 26th International Congress of the Aeronautical Sciences (ICAS)*, International Congress of the Aeronautical Sciences Paper 2008-5.10.1, Stockholm, Sept. 2008.

[15] Masui, K., Tomita, H., and Yanagida, A., "Research and Development for Fault Tolerant Flight Control System, Part 2: Flight Experiments," *Proceedings of the 26th International Congress of the Aeronautical Sciences (ICAS)*, International Congress of the Aeronautical Sciences Paper 2008-5.10.2, Stockholm, Sept. 2008.

[16] Miettinen, K., *Nonlinear Multiobjective Optimization*, Kluwer Academic, Boston, 1999.

[17] Prats, X., Puig, V., Quevedo, J., and Nejjari, F., "Lexicographic Optimisation for Optimal Departure Aircraft Trajectories," *Aerospace Science and Technology*, Vol. 14, No. 1, Jan.–Feb. 2010, pp. 26–37. doi:10.1016/j.ast.2009.11.003

[18] Prats, X., "Contributions to the Optimisation of Aircraft Noise Abatement Procedures," Ph.D. Thesis, Aerospace Science and Technology, Technical Univ. of Catalonia (UPC), Castelldefels, Spain, Jan. 2010.

[19] Stevens, B. L., and Lewis, F. L., *Aircraft Control and Simulation*, Wiley, London, 1992.

[20] ICAO, "*Manual of the ICAO Standard Atmosphere: Extended to 80 Kilometres (262,500 feet)*," 3rd ed., International Civil Aviation Organization, Montreal, Canada, 1993, Doc. 7488.

[21] Olmstead, J. R., Fleming, G. G., Gulding, J. M., Roof, C. J., Gerbi, P. J., and Rapoza, A. S., "Integrated Noise Model (INM) Version 6.0 Technical Manual," Federal Aviation Administration Office of Environment and Energy, Paper FAA-AEE-02-01 Washington, D. C., Jan. 2002.

[22] Zaheeruddin, V. J. K., and Guru, S. V., "A Fuzzy Model for Noise-Induced Annoyance," *IEEE Transactions on Systems, Man and Cybernetics, Part A: Systems and Humans*, Vol. 36, No. 4, 2006, pp. 697–705. doi:10.1109/TSMCA.2005.851348

[23] Botteldooren, D., Verkeyn, A., and Lercher, P., "A Fuzzy Rule Based Framework for Noise Annoyance Modeling," *Journal of the Acoustical Society of America*, Vol. 114, No. 3, 2003, pp. 1487–1498. doi:10.1121/1.1604125

[24] Prats, X., Puig, V., Quevedo, J., and Nejjari, F., "Multi-Objective Optimisation for Aircraft Departure Trajectories Minimising Noise Annoyance," *Transportation Research Part C: Emerging Technologies*, Vol. 18, No. 6, Dec. 2010, pp. 975–989.

[25] "Fuel Conservation Strategies: Cost Index Explained," *AERO Quarterly*, Quarter 2, The Boeing Co., Seattle, WA, 2007.

[26] Prats, X., Puig, V., Quevedo, J., and Nejjari, F., "Hierarchical and Sensitivity Analysis for Noise Abatement Departure Procedures," *Proceedings of the 8th AIAA Aviation Technology, Integration, and Operations (ATIO) Conference*, AIAA Paper 2008-8867, Sept. 2008.

[27] Rawls, J., *A Theory of Justice*, Belknap Press of Harvard Univ. Press, Cambridge, MA, 2005.

[28] Cunningham, E., "The Absolute Maximum Payoff in Differential Games and Optimal Control," *Journal of Optimization Theory and Applications*, Vol. 7, No. 4, 1971, pp. 258–286. doi:10.1007/BF00928707

[29] Miele, A., Mohanty, B., Venkataraman, P., and Kuo, Y., "Numerical Solution of Minimax Problems of Optimal Control, Part 1," *Journal of Optimization Theory and Applications*, Vol. 38, No. 1, 1982, pp. 97–109. doi:10.1007/BF00934325

[30] Aggarwal, R., and Leitmann, G., "A Maxmin Distance Problem," *Transactions of the ASME: Journal of Dynamic Systems, Measurement and Control*, Vol. 94, No. 2, 1972, pp. 155–158.

[31] Chen, M., "Individual Monotonicity and the Leximin Solution," *Economic Theory*, Vol. 15, No. 2, 2000, pp. 353–365. doi:10.1007/s001990050017

[32] "Girona (LEGE) Aerodrome Data," Aeronautical Information Publications (AIP): Part AD- LEGE, Aeropuertos Españoles y Navegación Aérea, Madrid, Oct 2009.

[33] ICAO, *Procedures for Air Navigation Services—Aircraft Operations (PANS-OPS), Volume I: Flight Procedures*, International Civil Aviation Org., Doc. 8168, Montreal, Canada, 5th ed., 2006.

[34] "Joint Aviation Requirements. JAR-OPS: Airplane Operations," Joint Aviation Authorities, Hoofddorp, The Netherlands, 2003.

[35] Pratt, R. W. (ed.), *Flight Control Systems: Practical Issues in Design and Implementation*, IEE Control Engineering Series, Institution of Engineering and Technology, Herts, U. K., March 2000.